2015

Nudged-elastic band method with two climbing images: Finding transition states in complex energy landscapes

Nikolai A. Zarkevich
Ames Laboratory, zarkev@ameslab.gov

Duane D. Johnson
Iowa State University, ddj@iastate.edu

Nudged-elastic band method with two climbing images: Finding transition states in complex energy landscapes

Abstract
The nudged-elastic band (NEB) method is modified with concomitant two climbing images (C2-NEB) to find a transition state (TS) in complex energy landscapes, such as those with a serpentine minimal energy path (MEP). If a single climbing image (C1-NEB) successfully finds the TS, then C2-NEB finds it too. However, improved stability of C2-NEB makes it suitable for more complex cases, where C1-NEB misses the TS because the MEP and NEB directions near the saddle point are different. Generally, C2-NEB not only finds the TS, but also guarantees, by construction, that the climbing images approach it from the opposite sides along the MEP. In addition, C2-NEB provides an accuracy estimate from the three images: the highest-energy one and its climbing neighbors. C2-NEB is suitable for fixed-cell NEB and the generalized solid-state NEB.

Keywords
Materials Science and Engineering, Density functional theory, Nickel, Shape memory effect, Optimization, Band structure

Disciplines
Engineering Physics | Metallurgy

Comments
C2-NEB code is available for download.

The following article appeared in *Journal of Chemical Physics* 142 (2015): 024106 and may be found at http://dx.doi.org/10.1063/1.4905209.

Nudged-elastic band method with two climbing images: Finding transition states in complex energy landscapes a)

Nikolai A. Zarkevich and Duane D. Johnson

Citation: The Journal of Chemical Physics **142**, 024106 (2015); doi: 10.1063/1.4905209
View online: http://dx.doi.org/10.1063/1.4905209
View Table of Contents: http://scitation.aip.org/content/aip/journal/jcp/142/2?ver=pdfcov
Published by the AIP Publishing

Nudged-elastic band method with two climbing images: Finding transition states in complex energy landscapes[a)]

Nikolai A. Zarkevich[1,b)] and Duane D. Johnson[1,2,c)]
[1]*Ames Laboratory, U.S. Department of Energy, Ames, Iowa 50011-3020, USA*
[2]*Department of Materials Science & Engineering, Iowa State University, Ames, Iowa 50011-2300, USA*

(Received 7 October 2014; accepted 17 December 2014; published online 9 January 2015)

The nudged-elastic band (NEB) method is modified with concomitant two climbing images (C2-NEB) to find a transition state (TS) in complex energy landscapes, such as those with a serpentine minimal energy path (MEP). If a single climbing image (C1-NEB) successfully finds the TS, then C2-NEB finds it too. However, improved stability of C2-NEB makes it suitable for more complex cases, where C1-NEB misses the TS because the MEP and NEB directions near the saddle point are different. Generally, C2-NEB not only finds the TS, but also guarantees, by construction, that the climbing images approach it from the opposite sides along the MEP. In addition, C2-NEB provides an accuracy estimate from the three images: the highest-energy one and its climbing neighbors. C2-NEB is suitable for fixed-cell NEB and the generalized solid-state NEB. © *2015 AIP Publishing LLC.* [http://dx.doi.org/10.1063/1.4905209]

I. INTRODUCTION

The Nudged-Elastic band (NEB) method has become a workhorse in determining the transition states (TS) and minimum-energy paths (MEPs) for both fixed-cell[2] and generalized solid-state transformations,[3] especially when implemented within density-functional theory (DFT). The available climbing-image algorithm, known as single climbing image (C1-NEB), is a modification of the NEB method,[4,5] where at each step, the highest-energy image (HEI) climbs. Here, to broaden the NEB applicability, we provide an extension to two climbing images (C2-NEB) method that is more stable and reliable for complex potential-energy landscapes.

In C2-NEB with two climbing images, both neighbors of the HEI climb towards TS, while the HEI is nudged to them. Hence, all three images move towards the TS saddle point, and the two climbing images are guaranteed to approach it along the MEP from opposite directions; their motion along the MEP provides higher stability compared to C1-NEB, with an accurate estimate of the TS energy from the three images. For a serpentine MEP (Fig. 1), C1-NEB can miss the TS, while C2-NEB does not require as many images as C1-NEB to find the correct result (Fig. 2), and naturally provides a denser grid of images near the saddle point, so it is more efficient and converges faster.

To showcase the method, we apply our C2-NEB code[1] implemented within DFT using VASP[6] to study deformations of the NiTi shape-memory alloy.[11] As illustrations, we consider a success (Fig. 3) and failure (Fig. 4) of the available C1-NEB algorithm. In the case of C1-NEB success, C2-NEB finds the same TS; whereas, for its failure, C2-NEB successfully finds the TS missed by C1-NEB. We further detail this using a simple 2-dimensional (2D) model, Figs. 1, 2, and 5. We conclude that our C2-NEB method is more stable and reliable, with a broader applicability.

II. METHOD

Our code[1] is implemented as follows. At each optimization step, the HEI is found. If this HEI is one of the two terminal points, then there is no climbing. If it is next to the fixed terminal point, then C1-NEB is used for this step. Finally, if the HEI does not coincide with the fixed ends or their direct neighbors, then C2-NEB algorithm is used for this step. Because the current HEI is determined at each step, the climbing images (and even the algorithm) can change from step to step. These changes of the HEI index will slow convergence; however, they do not affect the final converged result. As we prove below, upon convergence, the climbing images are guaranteed to bracket the saddle from both sides in C2-NEB.

Formally, let N moving images be enumerated from 1 to N, while the two fixed terminal images have indices 0 and $(N+1)$. At each step, the index M of the HEI is found. In this notation, our algorithm can be presented by the following pseudo-code.

At each optimization step, the algorithm is chosen:

- if $1 < M < N$, then C2-NEB;
- else, if $M = 1$ or $M = N$, then C1-NEB;
- else, NEB without climbing.

Each image I decides if it is climbing at this step.

- For C2-NEB, if $I = (M-1)$ or $I = (M+1)$, then climbing; else nudged (not climbing).
- For C1-NEB, if $I = M$, then climbing; else nudged.

In a NEB without climbing, every image is nudged.

[a)]C2-NEB code is available for download.[1]
[b)]Electronic mail: zarkev@ameslab.gov
[c)]Electronic mail: ddj@ameslab.gov

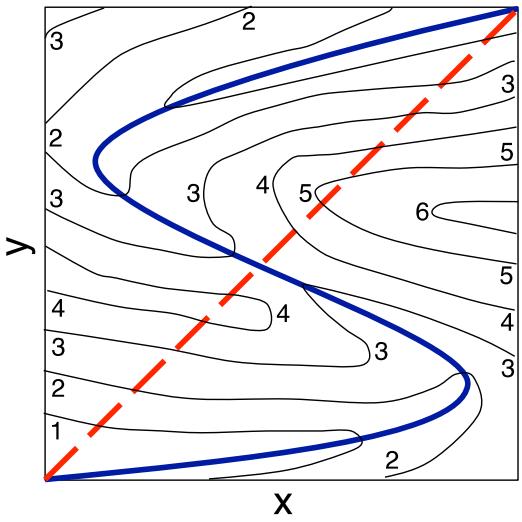

FIG. 1. Serpentine MEP (solid blue curve) example and a sparse-image NEB direction (dashed red line) near the TS saddle point. Energy isosurfaces, in arbitrary relative units, are for a system with two degrees of freedom (x, y).

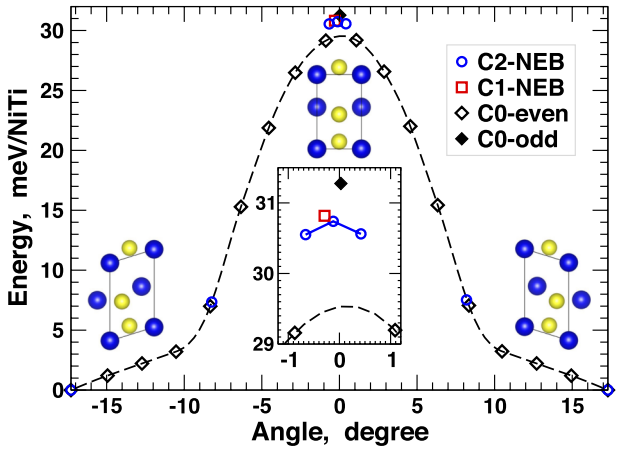

FIG. 3. Deformation energy for BCO-NiTi[8] versus angle between lattice vector a and normal to (bc) plane for algorithms: 5-image C2-NEB (blue circles); 1-image C1-NEB (red square); and non-climbing SS-NEB with even (C0-even, open diamonds) and odd (C0-odd, filled diamond) number of images. Inset: enlarged near TS. Unit cells of TS (B19) and BCO (B19') structures with Ni (yellow) and Ti (blue) atoms.

Convergence criteria in C2-NEB are chosen to be identical to those in C1-NEB, i.e., specified tolerances for the atomic forces, pressure components, and step-to-step enthalpy differences for all images. Of course, the convergence tolerance cannot be less than permitted by accuracy of the underlying force method, as discussed below for DFT-based applications.

Convergence behavior of the algorithm is defined as a sequence of optimization steps, during which the HEI index does not change; the energy differences between the HEI and each climbing neighbor are decreasing as optimization progresses, stopping after achieving the specified convergence criteria for all images. We can state unequivocally: *In C2-NEB, nearing convergence, if the HEI index does not change, then two climbing images approach the HEI from the opposite directions near the saddle*. This statement holds true by construction; otherwise, with both climbing images on one side, the nudged image will move to an energy between those of its neighbors (i.e., no longer the maximal one) and, hence, the index of the HEI will change at the next step and the statement again holds true.

For the community, our C2-NEB code[1] is available as a replacement of file `neb.F` in the NEB code.[2] We combine C2-NEB with DFT implemented in VASP.[6] The climbing is turned on by setting LCLIMB=.TRUE. in the INCAR file.[6] As implemented,[1] the C2-NEB convergence criteria are identical to those in C1-NEB. In C2-NEB, the small remaining distribution of energies and atomic coordinates upon convergence of 3 images (the HEI and two climbing ones) to the TS provides additional useful information.

III. APPLICATIONS

We apply C2-NEB to study (A) a deformation of the martensitic structure in the NiTi shape-memory alloy;[7–11] (B) its more complicated transformation to the austenite; and

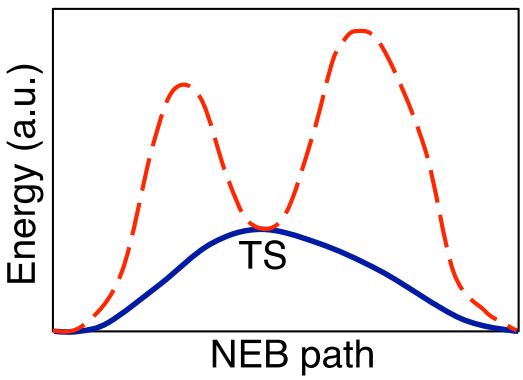

FIG. 2. Energy (arbitrary units) along the NEB path near TS in a C2-NEB (solid blue) and sparse-image C1-NEB (dashed red) algorithm. Due to different MEP and sparse-image NEB directions (Fig. 1), the saddle point is the energy maximum along the path in C2-NEB, but not in a sparse-image C1-NEB.

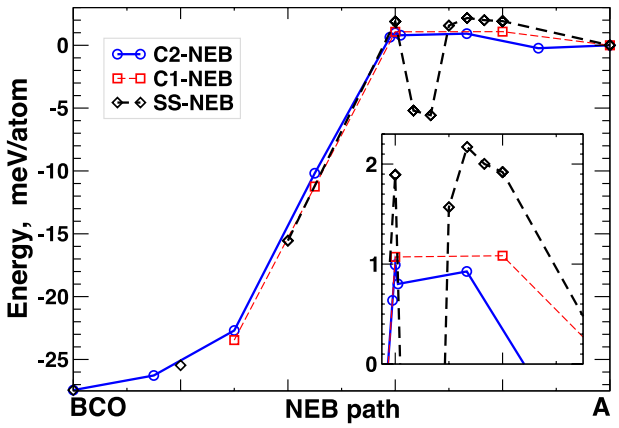

FIG. 4. Energy (meV/atom) relative to austenite (A) for the martensitic transformation in NiTi from the low-T BCO[8] to the high-T austenite,[7] represented by a $Ni_{54}Ti_{54}$ unit cell with 324 degrees of freedom. C2-NEB finds the TS at 1 meV/atom. C1-NEB swaps the HEI and then diverges; shown here is the moment of this swap (not the final C1-NEB result). SS-NEB with 4 images overestimates the barrier; added images reveal intermediate minimum.

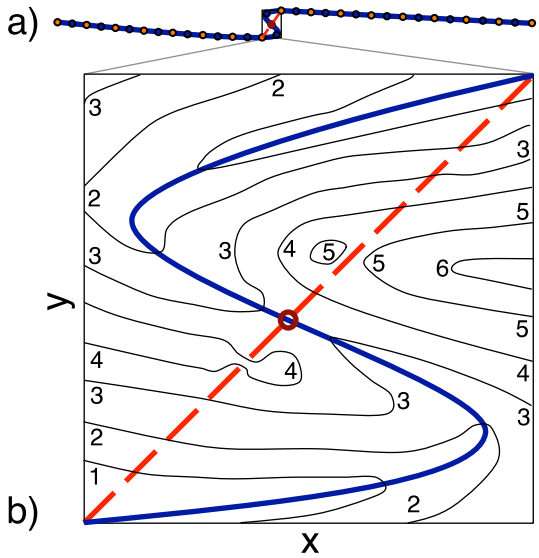

FIG. 5. (a) Example MEP (blue solid curve) with a zigzag near TS. (b) Enlargement near TS (red circle) differs from Fig. 1 by two extra higher-energy saddles in the potential energy surface, crossed by dashed red line. C1-NEB with 18 images [1 climbing (red) and 17 nudged (orange)] stops at a higher-energy saddle, not the TS. C1-NEB with 35 images (red, orange, and black dots) can find the TS with a good initial guess. C2-NEB with only 3 images converges to the TS.

(C and D) a 2D model (Figs. 1, 2, and 5) with a serpentine MEP. The DFT details are specified in Ref. 7.

We emphasize that the accuracy of the NEB implemented within DFT cannot exceed the DFT accuracy. Notably, to increase accuracy below this given accuracy within VASP, for example, requires excessive numbers of plane waves and can even decrease the possible unit-cell size for applications. In contrast to simple model potentials, one cannot achieve convergence to arbitrary accuracy to machine precision. Moving atoms and deforming a unit cell introduce nonsystematic errors,[12] preventing NEB convergence to an arbitrary accuracy. The limitation on accuracy must be taken into account when analyzing NEB results.

A. Deformation of the NiTi martensite

Equiatomic NiTi has a base-centered orthorhombic (BCO) ground state,[8] which is easily deformed into the observed B19' structure in the martensite. Deformation energies (Fig. 3) were obtained from the algorithms using the C2-NEB, C1-NEB, and solid-state NEB (SS-NEB) with an odd number of images without climbing. All methods give an energy barrier at 31 ± 0.5 meV/NiTi—the same answer within DFT error. Hence, in this simple case, C1-NEB is as good as C2-NEB. As expected,[2] SS-NEB with an even number of 16 images does not place any of them at the TS, which can be bypassed by the extrapolation. Again, this is a straightforward deformation without any significant twists in the MEP. Thus, C1-NEB with a single image provides sufficient accuracy. Adding more images increases computational cost, but does not improve the accuracy. C1-NEB with more images, C2-NEB, or a NEB with an odd number of images (no climbing) all give the same answer within the DFT error bar.

B. Complex energy landscape: NiTi martensite-to-austenite transformation

Considering the newly reported stable NiTi austenite,[7] a more complex structure with a hexagonal $Ni_{27}Ti_{27}$ primitive cell, we find that SS-NEB overestimates the barrier, while C1-NEB misses the TS for the austenite-to-martensite transition (Fig. 4). Calculations are performed in a 108-atom $Ni_{54}Ti_{54}$ unit cell, constructed from $Ni_{27}Ti_{27}$ primitive cell doubled along a, which transforms to 27 BCO 4-atom unit cells. This cell has 324 degrees of freedom that are coupled, making it computationally demanding as the number of NEB images increase, but still possible with a limited number of images in C2-NEB.

First, we used the SS-NEB[3] with 4 non-climbing images, and got a barrier above 2 meV/atom (Fig. 4). Later, additional detail was found by adding 5 more images between two fixed highest-energy ones; the valley between them is real (Fig. 4). Next, we use C1-NEB[2] with the same 4 images—the single climbing image swaps its index and then runs away to unreasonably high energies (the moment of this swap is shown in Fig. 4). We double the number of images and obtain the same result. We discard this diverged (unsuccessful) C1-NEB result. We then took the SS-NEB result, added more images as linear interpolations between available structures, and used C2-NEB with 8 images to find a barrier of 1 meV/atom. C2-NEB has 3 images at the TS (Fig. 4), including two climbing images and the HEI nudged to them. As a check, we combined those 3 C2-NEB images into one, and feed the result into the C1-NEB code. Given this initial configuration, C1-NEB moved images along its NEB path, swapped the HEI, and diverged again. Adding or removing a nudged image near the austenite did not stabilize C1-NEB and did not prevent the HEI swaps. Investigation of the second maximum with C2-NEB lowered its energy below 0.8 meV/atom; that maximum is similar to the one shown by dashed line in Fig. 2.

In both C2-NEB and C1-NEB, we find that each change of the HEI index slows down convergence, because all other (nudged) images try to rearrange equidistantly between the new climbing image and a fixed terminal state. In C1-NEB, a swap of the climbing HEI can change convergence to divergence, while C2-NEB is more stable. With sufficient accuracy at a lower computational cost, C2-NEB can be used with a small total number of images (minimum 3; we used 5 or more), while its 3 images approaching the TS create a dense grid at the right place, improving convergence and stability.

C. Serpentine MEP in two dimensions

Let us return to the 2-dimensional example in Fig. 1. For standard C1-NEB,[2] a single image tries to increase its energy by climbing along the path and decrease energy by relaxation in the transverse direction. Figure 2 shows an energy profile along a sparse-image NEB direction (the only saddle that has positive curvature along the NEB path and negative curvature in transverse direction). Placed near the TS, the C1-NEB climbing image will attempt to climb along the NEB path (dashed line in Fig. 1). The climbing image can stop only in a saddle with negative curvature along the NEB path, and,

if such a saddle is not present, then the convergence criteria will be never satisfied. Hence, after climbing away from the TS along the NEB path, the image will relax down to the serpentine MEP, move along the MEP towards the TS until it passes the curve, at which point, the image climbs from the MEP to higher energies, after which the image relaxes again to the serpentine MEP—a process that may never stop.

NEB with only a few images (no climbing) can also miss the correct answer.[2] With a sufficiently large number of images, NEB can find the saddle point. There is only one saddle in Fig. 1, and a NEB with a dense grid will find it, while C1-NEB with a dense grid will place one of the images at the saddle. C2-NEB always provides a denser grid of images at the right place near the saddle, allowing a smaller total number of images for convergence compared to C1-NEB and NEB without climbing. C2-NEB requires only 3 images to find the TS in Fig. 1.

D. Efficiency comparison for a serpentine MEP

To compare efficiency of C1- and C2-NEB, let us consider a model potential energy surface in the shape of a long valley with a zigzag near TS (Fig. 5), having a monotonically decreasing energy with distance from the TS along the valley bottom (Fig. 2, solid line). The region near TS in Fig. 5(b) differs from Fig. 1 by two additional higher-energy saddles.

For C1-NEB, a serpentine MEP presents a serious challenge. C1-NEB with 18 images placed initially along the MEP will not find the TS, because the climbing image placed near the TS climbs along the NEB path (dashed line in Fig. 5(b)) and stops at a higher-energy saddle (an energy maximum on the dashed line in Fig. 2). The climbing image in C1-NEB cannot (can) stop at a saddle that has an energy minimum (maximum) along the NEB path. However, with 35 images, C1-NEB can find the correct TS. In contradistinction, C2-NEB with only 3 images, placed equidistantly along the valley bottom as an initial guess, finds the TS. Hence, C2-NEB is much more efficient in this case. Accounting for failure of C1-NEB with up to 18 images, C2-NEB is also more reliable.

For completeness, we note that, in a system with multiple saddles, one can prepare an initial guess in such a way that both C1-NEB and C2-NEB will converge to another higher-energy saddle that is not on the MEP. NEB without climbing also will converge to the bottom of some valley, not necessarily the MEP, and extrapolation of energies between its images can miss the saddle.[2] In the example in Fig. 5, C1-NEB with 18 or fewer images cannot find the correct TS, while C2-NEB is successful with only 3 images.

IV. DISCUSSION

Looking back at the complex topology of the energy landscape in Sec. III B with multiple saddles and even more than one maximum along the path, we admit that even a dense-grid NEB with a very large number of images converges to a local stable solution, which might, however, differ from the global MEP in some cases. Depending on the initial guess, MEP can be missed, and increasing density of images near suspected saddle will not shift the whole path to a lower saddle. C2-NEB carefully reflects the area near the HEI, but retains all features of the traditional NEB away from the HEI; similarly, C2-NEB can even miss a higher barrier if there are multiple barriers along the same path and the highest one is not sampled by sparse images. C2-NEB provides an important improvement in the density of images near the HEI, and inherits the NEB features, leaving any problems away from the HEI unaffected.

We have shown that for a simple system (Sec. III A), C1-NEB with a single image can find the barrier, and C2-NEB with 3 images finds the same result; adding more images does not improve the accuracy. For a more complicated system with a serpentine MEP, C2-NEB becomes more efficient by providing higher density of images near the saddle, as we have proved by explicit example. In principle, a sufficient number of images in NEB (without climbing) or C1-NEB should provide the same result. Depending on the system complexity, this "sufficient number" changes from one for a simple transformation (Sec. III A) to a prohibitively large number for a serpentine MEP in a multidimensional space (Sec. III B). Due to a smaller number of images needed for convergence to the saddle point, C2-NEB is more efficient in more complex cases, achieving convergence for the same criteria as C1-NEB.

We note for completeness that in both C1-NEB and C2-NEB, all images away from the climbing ones converge towards equidistant distribution along the path. Each swap in the HEI index disrupts convergence and restarts the optimization process. Hence, in both algorithms, it is recommended first to achieve convergence of NEB without climbing, and only after that to switch on climbing. Upon switching to C2-NEB, one can add a couple of extra images on both sides of the HEI, because one climbing HEI in C1-NEB corresponds to 3 images in C2-NEB (the HEI and its two climbing neighbors).

V. SUMMARY

In summary, we have implemented a C2-NEB algorithm[1] to find reliably minimum-energy paths in complex potential-energy landscapes. We tested our C2-NEB method on the NiTi shape-memory transformations for martensite-to-martensite and austenite-to-martensite, with its serpentine minimum-energy path. By NiTi and model examples, we have shown that C2-NEB finds a transition state on a serpentine pathway even if C1-NEB misses it. If C1-NEB finds the TS, then C2-NEB finds it too with higher stability and additional image information. C2-NEB is more reliable than C1-NEB because the climbing images move along the minimum-energy path and form a denser grid of images near the transition state.

The implementation of the C2-NEB algorithm is provided as a useful modification of the existing NEB[2] and the generalized solid-state NEB[3] codes. The C2-NEB code is available as a replacement of `neb.F` file in the NEB code;[1] as implemented in VASP, the climbing is turned on by setting `LCLIMB=.TRUE.` in the INCAR file.[6]

ACKNOWLEDGMENTS

This work is supported by the U.S. Department of Energy, Office of Science, Basic Energy Sciences, Materials Science and Engineering Division. The research is performed at the Ames Laboratory, which is operated by Iowa State University under Contract No. DE-AC02-07CH11358.

[1]N. A. Zarkevich and D. D. Johnson, C2-NEB source code, http://lib.dr.iastate.edu/ameslab_software/1/.
[2]G. Henkelman and H. Jónsson, J. Chem. Phys. **113**, 9901-9904 (2000); **113**, 9978-9985 (2000), see http://theory.cm.utexas.edu/vtsttools/neb.html.
[3]D. Sheppard, P. Xiao, W. Chemelewski, D. D. Johnson, and G. Henkelman, J. Chem. Phys. **136**, 074103 (2012).
[4]G. Mills, H. Jónsson, and G. K. Schenter, Surf. Sci. **324**, 305 (1995).
[5]H. Jónsson, G. Mills, and K. W. Jacobsen, "Nudged elastic band method for finding minimum energy paths of transitions," in *Classical and Quantum Dynamics in Condensed Phase Simulations*, edited by B. J. Berne, G. Ciccotti, and D. F. Coker (World Scientific, 1998).
[6]G. Kresse and J. Furthmüller, Comput. Mater. Sci. **6**, 15 (1996); Phys. Rev. B **54**, 11169 (1996).
[7]N. A. Zarkevich and D. D. Johnson, Phys. Rev. B **90**, 060102R (2014).
[8]X. Y. Huang, G. J. Ackland, and K. M. Rabe, Nat. Mater. **2**, 307 (2003).
[9]W. J. Buehler, J. V. Gilfrich, and R. C. Wiley, J. Appl. Phys. **34**, 1475 (1963).
[10]F. E. Wang, W. J. Buehler, and S. J. Pickart, J. Appl. Phys. **36**, 3232 (1965).
[11]N. A. Zarkevich and D. D. Johnson, Phys. Rev. Lett. **113**, 265701 (2014).
[12]N. A. Zarkevich, E. H. Majzoub, and D. D. Johnson, Phys. Rev. B **89**, 134308 (2014).